Sonar-Based Iceberg-Relative AUV Navigation

Peter Kimball* and Stephen Rock*†
pkimball@stanford.edu, rock@stanford.edu
*Dept. of Aeronautics and Astronautics
Stanford University
496 Lomita Mall
Stanford, CA 94305
†Monterey Bay Aquarium Research Institute
7700 Sandholdt Road
Moss Landing, CA 95039

***Abstract*—AUVs have been operating under the ice for years. All of these systems have relied on combinations of dead-reckoning using inertial measurements, acoustic transponder networks, and/or velocity measurements from a Doppler velocity logger (both seafloor-relative and ice-relative) for navigation and control. These existing systems can be very accurate for operation under a stationary ice sheet, but they cannot provide ice-relative navigation accounting for the full motion of free-floating icebergs (especially rotation). Further, while some of these AUVs have collected sonar images of the underside of the ice, none has used these data for navigation.**

This paper explores the extension of sonar-based terrain-aided navigation techniques to enable an AUV to localize its position with respect to a moving and rotating iceberg. Terrain-navigation techniques provide drift-free position estimates with respect to mapped terrain and have been demonstrated for aircraft, missile, and numerous underwater vehicle applications. The availability of terrain-aided navigation would enable an AUV to return to sites of interest for sampling and serial observations.

In particular, this paper presents an approach to developing maps of the underside of icebergs that would be sufficient to enable autonomous localization and navigation for AUVs. The viability of this approach is demonstrated using data collected from a sideways-looking multibeam sonar system mounted on the R/V Nathaniel B. Palmer in Antarctica, June 2008. During data collection, the ship completed approximately 400 degrees of circumnavigation of a small ($<$1nmi^2) free-floating iceberg. Hence, data from the beginning and end of the experiment overlap the same section of the iceberg. These data are used to estimate parameters in a simple iceberg motion model, and the iceberg-relative ship track is then recovered by subtracting the estimated iceberg motion from the measured GPS track of the ship. Projection of the measured sonar ranges from the iceberg-relative ship track yields a self-consistent iceberg map, up to the accuracy of the estimated iceberg motion.

I. Introduction

Every year, icebergs break off of grounded ice sheets and are carried far from their birthplaces by wind and water currents. These traveling ecosystems are of great interest to science, but are relatively difficult and dangerous to approach, making them attractive targets for exploration by Autonomous Underwater Vehicles (AUVs).

This work was supported by grant ANT-0811399 from the National Science Foundation.

Operation in these under-ice environments requires that an AUV possess some capability of navigation with respect to the ice surface. Existing under-ice AUV navigation systems have typically relied on dead-reckoning using inertial measurements and/or velocity measurements from a Doppler sonar (both seafloor-relative and ice-relative). These systems have been used successfully to move between preprogrammed waypoints in horizontal inertial space, with depth determined by reactive terrain-following or obstacle avoidance behaviors. However, these existing systems cannot provide accurate ice-relative position estimates around free-floating, rotating icebergs. Specifically, accelerometers, gyros, and compasses provide information about how the AUV moves with respect to an inertial frame, not with respect to the ice. DVLs can measure ice-relative velocity measurements, but they cannot account for any rotation of the ice. Hence, extensions to the navigation system are required for these missions.

Like GPS and acoustic transponder networks, Terrain-Relative Navigation (TRN) techniques can be utilized to eliminate drift error from dead-reckoned navigation estimates and to measure the heading of a vehicle. TRN works by correlating incoming sonar measurements with pre-stored terrain maps. If such a terrain map could be made of the underside of a free-floating iceberg, AUVs could employ appropriately extended TRN algorithms to navigate with respect to the moving ice (see [1] for a benthic application). Developing and demonstrating experimentally a procedure to create these maps is the focus of the work presented here.

II. Background

A. AUV Navigation Beneath Sea Ice

The inherent difficulty of accessing the under-ice environment has driven an increase in the capability of AUVs to operate at high latitudes and under sea ice [2]. AUV navigation in this environment is made challenging by the inability of AUVs to obtain GPS navigation fixes while beneath ice, by the reduced performance of navigation instruments at high-latitudes [3], and by the hazardous presence of both ice and seafloor obstacles. Nevertheless, many successful AUV missions have been performed beneath sea ice. These missions

have all utilized some form dead-reckoning navigation, with a variety of drift-correction techniques.

In its Arctic configuration, MIT Sea Grant's Odyssey II vehicle used only angular rate and acceleration sensors to derive vehicle attitude and heading. Drift in this estimate was corrected by magnetic field intensity measurements in all three vehicle axes, however this was done post-mission and was not an aid to navigation. Position estimation for vehicle navigation was achieved through the use of pre-deployed long baseline (LBL) or ultrashort baseline (USBL) acoustic systems. In addition, Odyssey II used an acoustic homing beacon as a directional reference when returning to a recovery location. During successful deployment in the Beaufort Sea (Arctic), an upward-looking sonar on Odyssey II created a record of ice-draft above the vehicle's navigation track [4].

The Canadian AUV, Theseus, was designed to lay several kilometers of fiber-optic cable beneath arctic ice. Theseus navigated to predetermined position waypoints using dead-reckoning, based on acceleration measurements from an IMU and velocity measurements from bottom-pinging Doppler sonar. The dead-reckoned position estimate drifted at a rate of 0.5% of distance traveled (%DT). To achieve an order of magnitude improvement (0.05%DT) in navigation, the dead-reckoned estimate was updated with position fixes from multiple acoustic beacons, installed at pre-surveyed locations along the desired vehicle path [5].

In October 2001, the Monterey Bay Aquarium Research Institute operated the ALTEX AUV in the Arctic to test the operation of various navigation instruments at high latitudes. Dead-reckoning using bottom-pinging (or ice-pinging) Doppler sonar, the ALTEX vehicle achieved position error better than 0.05%DT, without the use of external navigation aids (such as an LBL array). Under-ice missions on this deployment were approximately 5km long [3].

In February 2002, a Cambridge team deployed a Martin 150 AUV in East Greenland pack ice to obtain the first AUV-based sidescan sonar imagery of arctic pack ice. The Martin Positioning (MARPOS) system relied on dead-reckoning integration of inertial accelerations, angular rates from a ring-laser gyro, and velocities from bottom-pinging Doppler sonar. This system achieved 0.1%DT horizontal error, as long as bottom-pinging was possible. The vehicle used differential GPS at the surface to obtain periodic position fixes [6]. Also, in April 2007, a Cambridge team used an ice-lanuched Gavia vehicle to obtain three-dimensional digital terrain maps of the underside of sea ice in the Beaufort Sea. This vehicle maintained a position estimate by dead-reckoning with ice-pinging Doppler sonar, and was recovered via a tether [7].

The British Autosub Under Ice (AUI) program has deployed the Autosub AUV under both Arctic and Antarctic sea ice. AUI missions in Greenland [8] and Antarctica [9] returned three-dimensional images of under-ice topography, taken with upward-looking swath sonar from the AUV. Autosub utilized reactive obstacle avoidance for these missions, but was navigated using dead-reckoning techniques in which velocity measurements were made using bottom-pinging or ice-pinging Doppler sonar. Autosub navigated to its recovery point by following a ship-deployed acoustic homing beacon. Development of the Autosub collision avoidance system, along with the loss of the first Autosub vehicle, highlights the potential value of ice-relative navigation estimates [10].

B. Terrain-Relative Localization and Navigation

TRN systems are used to eliminate accumulated drift error in vehicle position estimates by correlating terrain contour measurements with a-priori terrain maps. The Terrain Contour Matching (TERCOM) algorithm was one of the first implementations of this principle, and was used to correct drift in cruise missile navigation systems for many years [11]. Sequences of single-beam altitude measurements from along missile trajectories form the inputs to the TERCOM algorithm.

More recently, TRN techniques have been used (in place of GPS or acoustic transponder arrays) to correct drift error in underwater vehicle systems. Implementations have been fielded which provide real-time corrections to vehicle navigation, while others are used in post-processing [12]–[14]. In all implementations, the achievable precision and accuracy of the navigation estimates are limited by the resolution and quality of the a-priori map. Furthermore, the terrain in the operating area must have sufficient texture to be used in identifying vehicle position - TRN techniques provide no benefit over large areas of completely flat terrain.

C. Mapping and SLAM

The a-priori terrain maps used in underwater TRN algorithms come from a number of sources. Multibeam sonars can be carried aboard ships, towfish, remotely operated vehicles (ROVs), and AUVs. While their proximity to the seafloor allows submerged vehicles to obtain very high resolution sonar imagery, they often suffer from navigation errors far greater than the accuracy of the sonars they carry. The creation of self-consistent high-resolution bathymetric maps using these vehicles thus requires some means of eliminating or minimizing these errors. Some mapping operations do so by utilizing LBL arrays during data collection [15], [16]. In others, AUVs are programmed to follow self-intersecting trajectories, and terrain correlation at these intersection points is used in post-processing to perform adjustments to the estimated AUV trajectory [17], [18]. In all of these operations, the focus is on generating the best possible estimate of vehicle trajectory. The final terrain map is then produced by projecting measured sonar ranges from this best-estimate trajectory.

In the vast body of Simultaneous Localization and Mapping (SLAM) literature, there are many applications to sonar-equipped underwater vehicles. CMU and Stone Aerospace developed a full three-dimensional SLAM capability for the DEPTHX vehicle, which operates in flooded sinkholes and tunnels [19]. The bathymetric mapping post-processing algorithm used by WHOI in [18] is based on SLAM methodology. Range sensor scan-matching techniques are used not only for underwater sonars, but also for sonar and laser rangefinders on terrestrial mobile robots. The iterative closest point algorithm (ICP) [20] and its variants have been used in a multitude of mobile robot SLAM applications such as [21], [22], as well as in 3D reconstruction work by the computer vision community.

Scan matching based on nearest-neighbor distances appears in much of this literature, and is used here for terrain correlation.

III. Method

A key step in enabling sonar-based navigation with respect to a moving ice surface is the creation of a self-consistent map of that surface. Self-consistent maps are those in which multiple sonar scans of the same terrain feature all result in that feature appearing at the same location in the map.

A. Approach

The procedure used here to create a self-consistent map is conceptually similar to the post-processing approach used in existing bathymetric mapping systems, such as MBSystem [23]. First, a best estimate of the mapping vehicle's trajectory is formed. Next, the sonar vectors recorded during the mission are projected from their appropriate origins along the vehicle trajectory into a common map reference frame (often latitude/longitude or universal transverse mercator). Finally, this point cloud map of sonar hits can be used to create a model of the terrain (often a grid of average elevation values, with interpolated values filling gaps in coverage).

For bathymetric mapping applications, a best estimate of the vehicle's trajectory can be generated by using terrain correlations at trajectory self-intersectons to compute a series of adjustments to a baseline navigation estimate. This baseline estimate is usually dead-reckoned using inertial accelerometers or ground-pinging Doppler sonar, and must be corrected because it suffers from accumulated drift error. The navigation correction algorithm uses terrain correlation to compute navigation adjustments at trajectory self-intersections. The best-estimate trajectory is then formed by enforcing these adjustments at trajectory self-intersections, and smoothing the baseline trajectory between them.

For underice applications (e.g. moving icebergs), this procedure must be extended to include an estimate of the motion of the surface being mapped. Specifically, the common map reference frame into which all sonar measurements are projected must be attached to the iceberg, and the best estimate of the vehicle trajectory must therefore be defined in this frame. Since the ice translates and rotates, the iceberg frame is non-inertial. However, the baseline vehicle trajectory estimate still describes the vehicle's motion in inertial space because it is dead-reckoned using inertial accelerations and an inertial heading reference.

The technique used here to account for this is to assume an iceberg motion model and to identify the values of parameters in the model based on ice surface correlation at trajectory self-intersections. Specifically, the model consists of the Northerly, Easterly, and heading speeds of the iceberg (note that a more complicated motion model can be included if required). Any choice of values for these parameters results in a unique iceberg-relative vehicle trajectory estimate and therefore a unique point cloud map. The self-consistency of this map is then measured at trajectory self-intersections with a simple nearest-neighbor-distances-squared cost function. The best-estimate trajectory is then the one resulting in the map of lowest self-consistency cost.

Given this best estimate of vehicle trajectory with respect to the ice, the remainder of the mapping procedure is unaffected. The sonar data are projected from the trajectory into the ice-fixed frame to create a point cloud map of the iceberg. From this point cloud map, a number of data reduction schemes could be used to create a model of the iceberg, but the point cloud itself is presented in this work.

B. Algorithm

At any time, t, the position of the vehicle with respect to the berg, $\vec{x}_{v/b}$, is given by (1).

$$\vec{x}_{v/b}(t) = \vec{x}_{v/I}(t) - \vec{x}_{b/I}(t) \tag{1}$$

Where $\vec{x}_{v/I}(t)$ is the position of the vehicle in inertial space, and $\vec{x}_{b/I}(t)$ is the position of the iceberg in inertial space.

Let $\hat{x}_{v/I}(t) = \vec{x}_{v/I}(t) + \vec{\epsilon}_{v/I}(t)$ be the baseline estimate of the vehicle trajectory in inertial space, made with error, $\vec{\epsilon}_{v/I}(t)$. Let $\hat{x}_{b/I}(t) = \vec{x}_{b/I}(t) + \vec{\epsilon}_{b/I}(t)$ be the assumed motion of the iceberg, with error, $\vec{\epsilon}_{b/I}(t)$. Then, the iceberg-relative trajectory estimate is given by (2).

$$\hat{x}_{v/b}(t) = \hat{x}_{v/I}(t) - \hat{x}_{b/I}(t) - \vec{\epsilon}_{v/I}(t) + \vec{\epsilon}_{b/I}(t) \tag{2}$$

Equation (3) defines the constant velocity iceberg motion model.

$$\dot{\hat{x}}_{b/I} = \begin{bmatrix} \dot{x}_{b_N} \\ \dot{x}_{b_E} \\ \dot{\psi}_b \end{bmatrix}, \ddot{\hat{x}}_{b/I} \equiv 0 \tag{3}$$

Where $\dot{x}_{b_N}$ is the iceberg Northerly velocity, $\dot{x}_{b_E}$ is the iceberg Easterly velocity, and $\dot{\psi}_b$ is the iceberg heading rate, all in inertial space. Note that $\hat{x}_{v/b}(t)$ depends on the parameters in this model, as well as on any parameters included to model the error terms, $\vec{\epsilon}_{v/I}(t)$ and $\vec{\epsilon}_{b/I}(t)$.

Define $M_k(\hat{x}_{v/b})$ as the projection of the k^{th} sonar ping, $Z(k)$, into the map frame under the estimated iceberg-relative vehicle trajectory, $\hat{x}_{v/b}$, as defined in (4) for $k \in 1, 2, ..., p$.

$$M_k(\hat{x}_{v/b}) = \hat{x}_{v/b}(t_k) + T(\hat{x}_{v/b}(t_k))Z(k) \tag{4}$$

Where $T(\hat{x}_{v/b}(t_k))$ is the transformation matrix from the vehicle frame to the iceberg frame at the time, t_k of the k^{th} ping, and p is the total number of pings in the data set.

Define two groups of pings, $pass1$ and $pass2$, such that at all trajectory self-intersections, the area of iceberg surface imaged in $pass2$ is completely subsumed by the area imaged in $pass1$. Compute the projections of these pings into the map frame as given by (5) and (6).

$$M_{pass1}(\hat{x}_{v/b}) = M_k(\hat{x}_{v/b}) \quad \text{for } k \in pass1 \tag{5}$$

$$M_{pass2}(\hat{x}_{v/b}) = M_k(\hat{x}_{v/b}) \quad \text{for } k \in pass2 \tag{6}$$

For each of the n points in $Mpass2$, find the closest point in $Mpass1$. Populate an n-length vector, $d_{NN}(\hat{x}_{v/b})$ with the distances between these nearest-neighbor pairs. The self-consistency cost, $J(\hat{x}_{v/b})$, associated with the iceberg-relative vehicle trajectory estimate is the average squared distance between nearest neighbor pairs, given by (7).

$$J(\hat{x}_{v/b}) = \tfrac{1}{n}\|d_{NN}\|^2 \tag{7}$$

The best-estimate iceberg-relative vehicle trajectory is the one which minimizes $J(\hat{x}_{v/b})$. The associated point cloud iceberg map is given by (4).

IV. Experimental Results

A. The Data Set

In June 2008, multibeam sonar mapping data were taken from an iceberg in the Scotia Sea. During data collection, the berg translated at approximately 0.09m/s (0.18kts), and rotated at approximately -26.6deg/hr. The sonar data were recorded by a sideways-looking 400KHz Reson multibeam sonar head, mounted on a pole 10m beneath the R/V Nathaniel B Palmer (see Fig. 1). The ship's track in inertial space was measured by GPS. Sonar imagery of the shallowest 250m (approximately) of the iceberg's submerged perimeter was collected as the ship made a steady 400° circumnavigation of the berg. Thus, the trajectory has a self-intersection, and the sonar imagery at the beginning and end of the data set represent the same portion of the iceberg surface. Data collection lasted just under 40 minutes. The iceberg appears in Fig. 2.

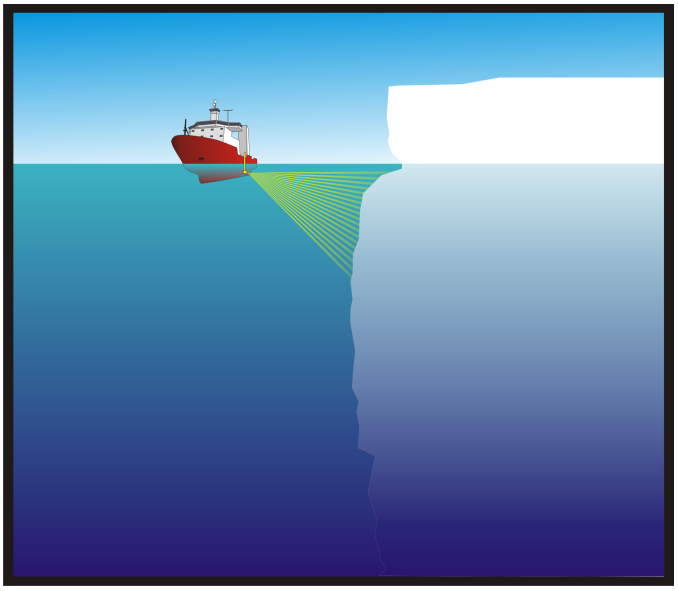

Fig. 1. Sideways-looking multibeam sonar beneath the R.V. Nathaniel B Palmer

B. Data Processing

Each multibeam sonar ping is tagged with the orientation and GPS position of the ship at the time of the ping. Raw sonar data were edited using the open-source, NSF-supported MB-System software package. Bad beams (e.g. max range, zero range, or excessive noise) were flagged using MB-System.

C. Navigation Estimation by Terrain Correlation

In this data set, there is a single trajectory self-intersection where the beginning and end of the trajectory overlap (this defines the points comprising $pass1$ and $pass2$). The baseline vehicle navigation estimate was the GPS measurement of the ship's ground track, and since the GPS error was assumed

Fig. 2. Photograph of iceberg represented in the data set

to be very small compared to iceberg motion during data collection, $\vec{\epsilon}_{v/I}(t)$ is assumed to be zero. Finally the iceberg's velocities were assumed to be constant, so $\vec{\epsilon}_{b/I}(t)$ is assumed to be zero as well. Note that while the shortcomings of the iceberg motion model are likely more significant than errors in the GPS estimate of ship position, neither of these two error terms is truly zero, and these errors will have a slight effect on the quality of the map produced.

The motion of this iceberg is clearly visible in Fig. 3, as pings from $pass1$ and $pass2$ lie tens of meters apart from one another.

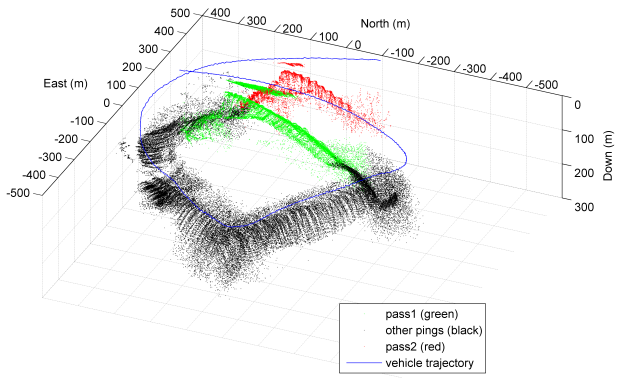

Fig. 3. Iceberg map derived from GPS vehicle navigation with no consideration of ice motion

Because of the assumptions that $\vec{\epsilon}_{v/I}(t)$ and $\vec{\epsilon}_{b/I}(t)$ are negligible, the only parameters estimated in this example are those of the iceberg motion model. The iceberg motion parameters which minimize the self-consistency cost are $\dot{x}_{b_N} = 0.0393m/s$, $\dot{x}_{b_E} = -0.0830m/s$, and $\dot{\psi}_b = -26.61deg/hr$. Based on this iceberg motion, a best estimate of iceberg-relative vehicle navigation, $\vec{x}_{v/b}$, and associated point cloud map have been recovered and appear in Fig. 4. To show the

overlapping area in more detail, the map projections $Mpass1$ and $Mpass2$ are plotted in Fig. 5.

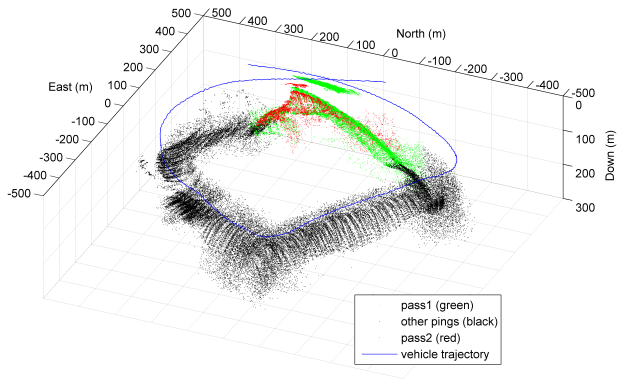

Fig. 4. Corrected iceberg map derived from iceberg-relative vehicle navigation estimate

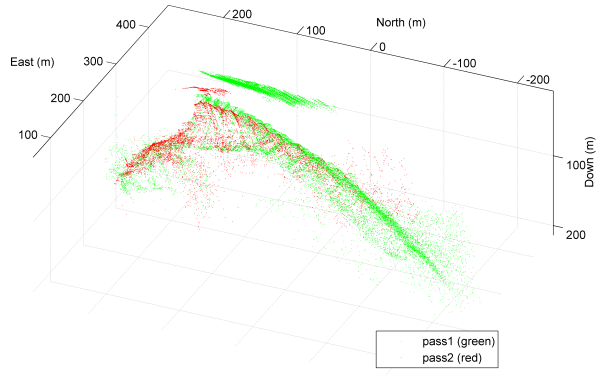

Fig. 5. Overlapping portion of corrected iceberg map

Overall, the resulting map (Fig. 4) shows dramatic improvement in self-consistency over the map created neglecting iceberg motion (Fig. 3). A small group of points appears at a different distance from the main berg in $pass1$ than it does in $pass2$. It is believed that these points represent a small chunk of ice which moves independently of the main berg. Inclusion of these points in the data set is a violation of the assumption that the ice surface does not change shape over the duration of data collection, and results in a slight misalignment of $Mpass1$ and $Mpass2$ (visible in Fig. 5).

In order to illustrate the behavior of the self-consistency cost function presented here, the cost was calculated over a three-dimensional grid of iceberg motion model parameters near the optimum. Calculated values of $J(\hat{x}_{v/b})$, for this exercise are presented in Fig. 6 (for three choices of heading rate). The shapes of the surfaces indicate that convergent search techniques, such as Iterative Closest Point, could be effective in quickly locating global optima in the space of iceberg motion model parameters.

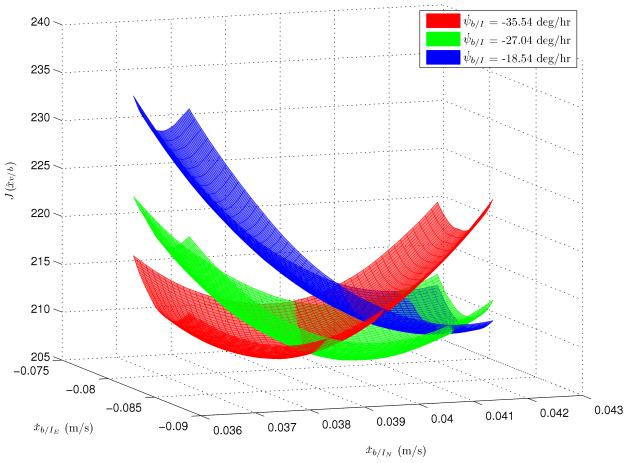

Fig. 6. Behavior of nearest-neighbor distance squared cost function

V. Conclusion

Extending the use of sonar to enable vehicle navigation with respect to free-floating icebergs requires two capabilities. First, the vehicle must be able to create a map of the ice surface of sufficient quality to represent a consistent world model. Second, in real time, the AUV must be able to correlate sonar measurements against the map in order to localize its current position. This work addresses the mapping task, presenting an extension to existing bathymetric mapping methods which uses terrain matching techniques with multibeam sonar data at trajectory self-intersections to evaluate choices of parameter values in an iceberg motion model. A simple nearest-neighbors cost function is used for this evaluation. The accuracy of the proposed method depends upon the ability of the iceberg motion model to describe accurately the true iceberg motion, on the quality of the baseline inertial vehicle navigation estimate, and on the existence of sufficient texture for correlation on the ensonified ice surface.

Experimental results were presented for ship-based sideways-looking multibeam sonar data, collected during circumnavigation of a small iceberg in the Scotia Sea. The experimental data include GPS position and time information. The point cloud iceberg map generated using the presented method shows dramatically improved self-consistency over the map created neglecting iceberg motion. By way of a grid search, it was also shown that the presented cost function is smooth and everywhere decreasing toward the global minimum.

Finally, it should be noted that while the experimental data used here were acquired by a ship using GPS, the results are applicable to AUVs equipped with inertial sensors. Both platforms have knowledge of their own position in inertial space, but lack the ability to navigate with respect to the moving ice. Even as AUVs venture beneath icebergs, looking upward at their targets, iceberg translational velocities and heading rates remain the parameters which must be estimated.

AUVs equipped with Doppler sonar may be able to measure translational velocities directly and often. For some operations (e.g. larger icebergs), the time between trajectory self-intersections will be increased, and more complex iceberg motion models may be required.

ACKNOWLEDGMENT

The authors would like to thank Reson Inc for the use of their 7125 sonar system. We would also like to thank Brett Hobson for deploying and operating the sonar system, Joanna O'Neill for collecting and processing the multibeam data, and Dave Caress for his expertise and help with MBSystem.

REFERENCES

[1] Debbie Meduna, Stephen Rock, and Rob McEwen, "Low-cost terrain relative navigation for long-range auvs", in *OCEANS*. MTS/IEEE, September 2008.

[2] Nicole Tervalon and Richard Henthorn, "Ice profiling sonar for an auv: Experience in the arctic", in *OCEANS*. MTS/IEEE, October 2002, vol. 1, pp. 305–310.

[3] Rob McEwen, Hans Thomas, Don Weber, and Frank Psota, "Performance of an auv navigation system at arctic latitudes", *IEEE Journal of Oceanic Engineering*, vol. 30, no. 2, pp. 443–454, April 2005.

[4] J.G. Bellingham, C.A. Goudey, T.R. Consi, J.W. Bales, D.K. Atwood, J.J. Leonard, and C. Chryssostomidis, "A second generation survey auv", in *Symposium on Autonomous Underwater Vehicle Technology*. AUV Technology, July 1994, pp. 148–155.

[5] Bruce Butler and Ron Verrall, "A precision hybrid inertial/acoustic navigation system for a long-range autonomous underwater vehicle", in *AM 98*. Institute of Navigation, 1998, pp. 561–572.

[6] P. Wadhams, J. P. Wilkinson, and A. Kaletzky, "Sidescan sonar imagery of the winter marginal ice zone obtained from an auv", *AMS Journal of Atmospheric and Oceanic Technology*, vol. 21, pp. 1462–1470, 2004.

[7] P. Wadhams and MJ Doble, "Digital terrain mapping of the underside of sea ice from a small AUV", *Geophysical Research Letters*, vol. 35, no. 1, 2008.

[8] P. Wadhams, J.P. Wilkinson, and S.D. McPhail, "A new view of the underside of arctic sea ice", *Geophysical Research Letters*, vol. 33, February 2006.

[9] K. W. Nicholls, E. P. Abrahamsen, J. J. H. Buck, P. A. Dodd, C. Goldblatt, G. Griffiths, K. J. Heywood, N. E. Hughes, A. Kaletzky, G. F. Lane-Serff, S. D. McPhail, N. W. Millard, K. I. C. Oliver, J. Perrett, M. R. Price, C. J. Pudsey, K. Saw, K. Stansfield, M. J. Stott, P. Wadhams, A. T. Webb, and J. P. Wilkinson, "Measurements beneath an antarctic ice shelf using an autonomous underwater vehicle", *Geophysical Research Letters*, vol. 33, April 2006.

[10] M. Pebody and Robert Sutton, "Autonomous underwater vehicle collision avoidance for under-ice exploration.", *Proceedings of the Institution of Mechanical Engineers – Part M – Journal of Engineering for the Maritime Environment*, vol. 222, no. 2, pp. p53 – 66, 20080501.

[11] J. P. Golden, "Terrain contour matching (tercom) - a cruise missile guidance aid", in *Image Processing for Missile Guidance*. SPIE, July 1980, vol. 238, pp. 10–18.

[12] Ingemar Nygren and Magnus Jansson, "Terrain navigation for underwater vehicles using the correlator method", *IEEE Journal of Oceanic Engineering*, vol. 29, no. 3, pp. 906–915, July 2004.

[13] Ryan Eustice, Richard Camilli, and Hanumant Singh, "Towards bathymetry-optimized doppler re-navigation for auvs", in *OCEANS*. MTS/IEEE, 2005, vol. 2, pp. 1430–1436.

[14] S. Williams and I. Mahon, "A terrain-aided tracking algorithm for marine systems", *The International Conf on Field and Service Robotics*, pp. 112–118, 2003.

[15] Vicki Lynn Ferrini, Daniel J. Fornari, Timothy M. Shank, James C. Kinsey, Maurice A. Tivey, S. Adam Soule, Suzanne M. Carbotte, Louis L. Whitcomb, Dana Yoerger, and Jonathan Howland, "Submeter bathymetric mapping of volcanic and hydrothermal features on the East Pacific Rise crest at 950degN", *Geochemistry, Geophysics, and Geosystems*, vol. 8, no. 1, January 2007.

[16] Dana R. Yoerger, Michael Jakuba, and Albert M. Bradley, "Techniques for deep sea near bottom survey using an autonomous underwater vehicle", *International Journal of Robotics Research*, vol. 26, no. 1, pp. 41–54, January 2007.

[17] WJ Kirkwood, "Development of the DORADO mapping vehicle for multibeam, subbottom, and sidescan science missions: Research Articles", *Journal of Field Robotics*, vol. 24, no. 6, pp. 487–495, 2007.

[18] Chris Roman and Hanumant Singh, "Improved vehicle based multibeam bathymetry using sub-maps and slam", in *Intelligent Robots and Systems*. IEEE/RSJ International, Aug 2005, pp. 3662– 3669.

[19] N. Fairfield, G. Kantor, and D. Wettergreen, "Real-Time SLAM with Octree Evidence Grids for Exploration in Underwater Tunnels", *JOURNAL OF FIELD ROBOTICS*, vol. 24, no. 1-2, pp. 3, 2007.

[20] P.J. Besl and N.D. McKay, "A Method for Registration of 3-D Shapes", *IEEE Transactions on Pattern Analysis and Machine Intelligence*, vol. 14, no. 2, pp. 239–256, 1992.

[21] A. Nuchter, H. Surmann, K. Lingemann, J. Hertzberg, and S. Thrun, "6D SLAM with an application in autonomous mine mapping", *Robotics and Automation, 2004. Proceedings. ICRA'04. 2004 IEEE International Conference on*, vol. 2, 1926.

[22] D. Hahnel and W. Burgard, "Probabilistic Matching for 3D Scan Registration", *Proc. of the VDI-Conference Robotik*, vol. 2002, 2002.

[23] D. Caress and D. Chayes, "Optimal Navigation Adjustment for Poorly Navigated Swath Bathymetry Surveys", *Eos Trans. AGU*, vol. 81, pp. 48, 2000.